Proc. Natl. Acad. Sci. USA
Vol. 96, pp. 5728–5733, May 1999
Medical Sciences

Suppression of angiogenesis and tumor growth by the inhibitor K1–5 generated by plasmin-mediated proteolysis

(angiostatin/plasminogen/antitumor)

RENHAI CAO*, HUA-LIN WU†, NIINA VEITONMÄKI*, PHILIP LINDEN‡, JACOB FARNEBO*, GUEY-YUEH SHI†, AND YIHAI CAO*§

*Laboratory of Angiogenesis Research, Microbiology and Tumor Biology Center, Karolinska Institute, S-171 77 Stockholm, Sweden; †Department of Biochemistry, National Cheng Kung University Medical College, Tainan, Taiwan, 70101, Republic of China; and ‡Department of Surgery, Brigham and Women's Hospital, Harvard Medical School, 300 Longwood Avenue, Boston, MA 02115

Edited by Judah Folkman, Harvard Medical School, Boston, MA, and approved January 28, 1999 (received for review August 21, 1998)

ABSTRACT **Proteolytic enzymes are involved in generation of a number of endogenous angiogenesis inhibitors. Previously, we reported that angiostatin, a potent angiogenesis inhibitor, is a proteolytic fragment containing the first four kringle modules of plasminogen. In this report, we demonstrate that urokinase-activated plasmin can process plasminogen to release an angiogenesis inhibitor, K1–5 (protease-activated kringles 1–5). K1–5 inhibits endothelial-cell proliferation with a half-maximal concentration of approximately 50 pM. This inhibitory effect is endothelial-cell-specific and appears to be at least approximately 50-fold greater than that of angiostatin. A synergistic efficacy of endothelial inhibition was observed when angiostatin and kringle 5 (K5) were coincubated with capillary endothelial cells. The synergistic effect is comparable to that produced by K1–5 alone. Systemic treatment of mice with K1–5 at a low dose significantly blocked the fibroblast growth factor-induced corneal neovascularization, whereas angiostatin had no effect at the same dose. K1–5 also suppressed angiogenesis in chicken embryos. Systemic administration of K1–5 at a low dose at which angiostatin was ineffective significantly suppressed the growth of a murine T241 fibrosarcoma in mice. The antitumor effect correlates with the reduced neovascularization. These findings suggest that the plasmin-mediated proteolysis may be involved in the negative switch of angiogenesis.**

Angiogenesis, the outgrowth of new capillaries from preexisting vessels, is essential for wound healing, female reproduction, embryonic development, organ formation, tissue regeneration, and tissue remodeling (1–3). Angiogenesis is a complex multistep process that includes endothelial proliferation, migration and differentiation, degradation of extracellular matrix, tube formation, and sprouting of new capillary branches (4). The complexity of the angiogenic process suggests the existence of multiple controls of the system that can be temporarily turned on and off.

Under pathological conditions, a switch of the angiogenic phenotype by up-regulation of angiogenic factors and perhaps down-regulation of angiogenesis inhibitors often leads to progression of many diseases including tumor growth and diabetic retinopathy. Several recent studies have produced direct and indirect evidence in proof that tumor growth and metastasis are angiogenesis-dependent (5–10). To induce neovascularization, tumors often overexpress several angiogenic stimulators, including members of the fibroblast growth factor (FGF) (11) and the vascular endothelial growth factor/vascular permeability factor families (12, 13). Tumors may produce one or more of these angiogenic peptides that can synergistically stimulate tumor angiogenesis (14–16). Recent studies show that tumors also generate inhibitors of angiogenesis, including angiostatin and endostatin (5, 17–21). It is now believed that a switch of the angiogenic phenotype is dependent on a local change of the balance between angiogenic stimulators and inhibitors.

Accumulative data from different laboratories have recently shown that a number of angiogenesis inhibitors are fragments or cryptic domains of large protein molecules (22, 23). For example, angiostatin and endostatin are proteolytic fragments of plasminogen (Pgn) and collagen XVIII, respectively (5, 19). The 16-kDa N-terminal fragment of prolactin (24) and an N-terminally truncated platelet factor 4 (25) are potent angiogenesis inhibitors. In addition, a C-terminal fragment of matrix metalloprotease 2, named PEX, inhibits angiogenesis and tumor growth (26). In contrast, the intact parental molecules of these inhibitors lack inhibitory activity on endothelial cells and are not angiogenesis inhibitors. It is now becoming clear that the generation of endogenous inhibitors from large precursor proteins with distinct functions is a recurrent theme in suppression of angiogenesis. Thus, proteolytic processing plays a critical role in control of the switch of angiogenesis.

Angiostatin contains the first four disulfide-linked structures of Pgn, known as kringle structures (5, 27). Smaller fragments of angiostatin display differential effects on suppression of endothelial cell growth (17). For example, kringle 1 (K1) exhibits greater than 50% of inhibitory activity of angiostatin, whereas kringle 4 (K4) is an ineffective fragment (17). We have recently discovered that the K5 domain of Pgn is a specific inhibitor for endothelial-cell proliferation (23). In fact, K5 appears to be more potent than angiostatin on inhibition of capillary endothelial-cell proliferation.

In this paper, we provide further evidence that plasmin, a fibrinolytic serine protease, can convert its precursor molecule, Pgn, into an angiogenesis inhibitor, K1–5, that is structurally related to angiostatin. Systemic therapy with pure K1–5 disrupts tumor-induced angiogenesis and tumor growth.

MATERIALS AND METHODS

Reagents, Cells, and Animals. Bovine capillary endothelial (BCE) cells were kindly provided by Judah Folkman (Harvard Medical School) and maintained in DMEM with 10% heat-inactivated bovine calf serum, antibiotics, and recombinant human fibroblast growth factor 2 (FGF-2 or basic fibroblast growth factor; Scios Nova, Mountainview, CA; 3 ng/ml). Recombinant human fibroblast growth factor 1 was expressed and purified as described (28). Murine T241 fibrosarcoma tumor cells were maintained in culture in DMEM supple-

The publication costs of this article were defrayed in part by page charge payment. This article must therefore be hereby marked "*advertisement*" in accordance with 18 U.S.C. §1734 solely to indicate this fact.

PNAS is available online at www.pnas.org.

This paper was submitted directly (Track II) to the *Proceedings* office.
Abbreviations: K1–5, protease-activated kringle 1–5; Pgn, plasminogen; K5, kringle 5; FGF, fibroblast growth factor; FGF-2, fibroblast growth factor 2; BCE, bovine capillary endothelial; CAM, chorioallantoic membrane.
§To whom reprint requests should be addressed. e-mail: yihai.cao@mtc.ki.se.

mented with 10% fetal calf serum (HyClone) and antibiotics. Male 5- to 6-week-old C57BL6/J mice (MTC, Karolinska Institute) were acclimated and caged in groups of six mice or less. Animals were anesthetized in a methoxyflurane chamber before all procedures and killed with a lethal dose of CO_2. All animal studies were reviewed and approved by the animal care and use committee of the Stockholm Animal Board.

Preparation of Proteolytic Fragments of Human K1–5 and Angiostatin. Intact, N-terminal Glu[1]-Pgn was purified from outdated and citrated human blood plasma by affinity chromatography on L-lysine-Sepharose, with a gradient of the ligand 6-aminohexanoic acid (17). Approximately 40 mg of purified Glu[1]-Pgn in 4 ml of 0.1 M glycine buffer (pH 10.5) was incubated at 25°C with immobilized urokinase-activated plasmin (10 M Pgn in 1 M plasmin) for 14 h (29). After incubation, the sample was applied to a lysine-Sepharose column (1.0 × 30 cm) preequilibrated and washed with 1.0 M sodium phosphate buffer (pH 8.0). A peak containing micro-Pgn was detected in the flow-through fraction. K1–5 was eluted from the column with a 0–25 mM linear gradient of 6-aminocapronic acid (Sigma). The protein fraction containing K1–5 was further purified with a Sephadex G-75 column (2.6 × 90 cm). The purified K1–5 was dialyzed against distilled H_2O and lyophilized. The purity of K1–5 was analyzed by SDS/PAGE. The purified K1–5 was analyzed by N-terminal and C-terminal sequencing. Human angiostatin was prepared by digestion of Pgn with porcine elastase and purified by affinity chromatography on lysine-Sepharose 4B as described (17).

Endothelial-Cell Proliferation Assay. BCE cells were isolated as described (30). BCE cells were maintained in DMEM containing 10% heat-inactivated bovine calf serum (BCS) and recombinant human FGF-2 (3 ng/ml). Cells growing in gelatinized six-well plates were dispersed in 0.05% trypsin solution and resuspended with DMEM containing 10% BCS. Approximately 10,000 cells in 0.5 ml were added to each gelatinized well of 24-well plates and incubated at 37°C for 24 h. The medium was replaced with 0.5 ml of fresh DMEM containing 5% BCS, and samples of kringle structures in triplicates were added to each well. After a 30-min incubation, FGF-2 was added to a final concentration of 1 ng/ml. After 72 h incubation, cells were trypsinized, resuspended in Isoton II solution (Coulter), and counted with a Coulter counter.

Chicken Embryo Chorioallantoic Membrane (CAM) Assay. The CAM assay was carried out as described (31, 32). Three-day-old fertilized White Leghorn eggs (OVA Production, Sörgården, Sweden) were cracked, and chicken embryos with intact yolks were carefully placed in plastic Petri dishes (20 × 100 mm). After a 48-h incubation in 4% CO_2/96% air at 37°C, disks of methylcellulose containing various concentrations of K1–5 dried on nylon meshes of 4 × 4 mm were implanted on the CAMs of individual embryos. The nylon mesh disks were made by desiccation of 20 μl of 0.45% methylcellulose (in H_2O). After 48–72 h of incubation, embryos and CAMs were examined under a stereoscope for the formation of avascular zones in the field of the implanted disks.

Mouse Corneal Micropocket Assay. The mouse corneal assay was performed as described (27, 31, 33, 34). Seven-week-old male C57BL6/J mice (~20 g) were divided into three groups. The control group ($n = 5$) received daily subcutaneous injections of 100 μl of PBS, including an injection on the day before pellet implantation. The other two groups ($n = 5$) were subcutaneously injected once daily with K1–5 and angiostatin in 100 μl of PBS at the dose of 2 mg/kg, including pretreatment with the same dose the day before corneal implantation. Corneal micropockets were created with a modified von Craefe cataract knife in both eyes of each mice. Into each pocket, a pellet containing approximately 80 ng of FGF and sucrose aluminum sulfate (Bukh Meditec, Copenhagen, Denmark) coated with hydron polymer type NCC (IFN Sciences, New Brunswick, NJ) was implanted. The pellet was positioned approximately 1.5 mm from the corneal limbus. The maximal vessel length, clock hours, and the vascular area of corneas of all mice were measured, with a slit-lamp stereomicroscope at a magnification of ×15, on the sixth day after corneal implantation.

Tumor Studies in Mice. Male 6-week-old C57BL6/J mice were used for tumor studies. Approximately 1×10^6 murine T241 fibrosarcoma cells growing in logarithmic phase were harvested and resuspended in PBS, and a single cell solution in a volume of 100 μl was implanted subcutaneously in the middle dorsum of each animal. Five mice were used in the treated groups and five mice were used in the control groups. Systemic treatment by subcutaneous injections with either 100 μl of PBS or K1–5 (2–2.5 mg/kg) and angiostatin (2–2.5 mg/kg) in PBS was begun shortly after implantation of tumor cells and continued once daily for a total of 18–20 treatments. Visible tumors were present 72 h after implantation. Primary tumors were measured with digital calipers on the days indicated. Tumor volumes were calculated according to the formula: width^2 × length × 0.52 as reported (27).

Histology. Tumor-bearing C57BL6/J animals were killed by an overdose of methoxyflurane on day 20 after tumor cell implantation, and viable tumor tissues were resected and fixed with 4% formalin in PBS for 24 h. Tissues were imbedded in paraffin according to standard histological procedures (27, 31). The sections (5 μm thick) were processed and stained with a rabbit anti-human von Willebrand factor (Dako) antibody as described (27). Microvessels were counted in high-power fields (×40) in five randomly selected fields of tumors from four mice of each group.

RESULTS

Identification and Characterization of Proteolytic K1–5. Serine proteases have recently been reported to be involved in the generation of angiogenesis inhibitors such as angiostatin (35, 36). Plasmin is a serine protease and angiostatin is an internal fragment of Pgn. To further study the role of the Pgn–plasmin system in the control of the switch of angiogenesis, human Glu[1]-Pgn was digested with urokinase-activated plasmin (Fig. 1*A*). The proteolytic fragments were purified by affinity chromatography on lysine-Sepharose, followed by gel filtration through a Sephadex G-75 column. SDS-gel electrophoresis showed that a proteolytic fragment with a molecular mass of 55 kDa was purified to homogeneity (Fig. 1*B*). N- and C-terminal sequencing analyses showed that the cleavage sites of plasmin were dibasic amino acids between Lys[76] and Lys[77] at the N terminus and between Arg[529] and Lys[530] at the C terminus, respectively (Fig. 1*A*). Thus, this fragment contains the intact K1–4 and most of the K5 domains (K1–5) of Pgn, termed K1–5.

Inhibition of Endothelial-Cell Proliferation by K1–5. To investigate whether K1–5 could inhibit endothelial-cell proliferation, purified proteolytic K1–5 was incubated with BCE cells stimulated with FGF-2 at a concentration of 1 ng/ml. K1–5 inhibited BCE cell growth in a dose-dependent manner (Fig. 2*A*). The concentration of K1–5 required to reach 50% inhibition was approximately 50 pM and the maximal inhibition was observed at the concentration of 200 pM (Fig. 2*B*). Higher concentrations did not further increase the inhibitory effect of K1–5 (Fig. 2 *B* and *C*) on these cells. The half-maximal concentration appears to be at least 50-fold lower than that of proteolytic human angiostatin. In the presence of K1–5, the morphology of BCE cells appeared to be similar to that of untreated cells. In addition, cell proliferation can be rescued with FGF-2 stimulation after removal of K1–5 at a high concentration of 132 nM (Fig. 2*D*). These data suggested that K1–5 was not toxic to BCE cells even at a high concentration. The antiproliferative effect of K1–5 appeared to be endothelial-cell-specific because the concentration required for maximal inhibition of BCE cell proliferation was not inhibitory on several nonendothelial cells lines, including primary human fibroblasts, human retinal pigment cells, NIH 3T3 fibroblasts,

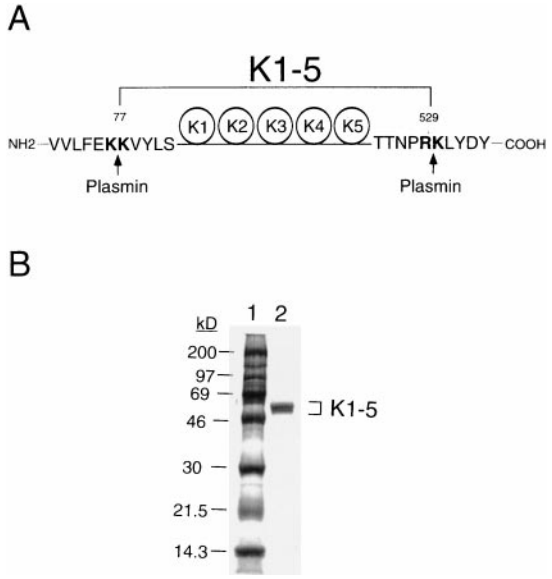

FIG. 1. Proteolytic fragment of human K1–5. (*A*) Plasmin cleavage sites. K1–5 fragment can be released by digestion of human Glu[1]-Pgn with urokinase-activated plasmin. N- and C-terminal sequencing analyses of purified K1–5 revealed that cleavage sites of plasmin were dibasic amino acids between Lys^{76} and Lys^{77} at the N terminus and between Arg^{529} and Lys^{530} at the C terminus, as indicated by arrows. K1–5 contains K1–4 and most part of K5 structures of Pgn. (*B*) SDS/PAGE analysis. The plasmin-digested K1–5 was purified by lysine-Sepharose affinity chromatography, followed by filtration through a Sephadex G-75 column. Four micrograms of purified protein were analyzed on a 10–20% gradient gel by SDS/PAGE under reducing conditions, followed by staining with Coomassie blue. K1–5 with molecular mass of 55 kDa was purified to homogeneity (lane 2). The molecular mass markers are indicated (in kDa) in lane 1.

rat smooth muscle cells, BHK cells, and T241 fibrosarcoma cells (data not shown).

Synergistic Inhibition of BCE Cell Proliferation by Angiostatin and K5. K5 of human and mouse Pgn has recently been reported to be a potent endothelial inhibitor (23). Because the structure of K1–5 contains angiostatin (K1–4) and K5, the enhancing effect of angiostatin and K5 on inhibition of BCE cell proliferation was tested. At the concentration of 1 nM, proteolytic human angiostatin did not significantly inhibit BCE cell proliferation, and less than approximately 50% of the inhibitory effect of BCE-cell proliferation by human proteolytic K5 was observed (Fig. 3). However, a synergistic efficacy of inhibition, which was approximately the maximal inhibition (>95%), was detected when both fragments at the concentration of 1 nM were added together to BCE cells. Interestingly, this synergistic inhibitory efficacy is comparable to that produced by K1–5 alone (Fig. 3*B*). High concentrations of K5 and angiostatin did not significantly show synergistic effects on suppression of BCE cell proliferation because K5 alone displayed nearly a maximal inhibition with increased concentrations (data not shown). These results demonstrate that angiostatin and K5 synergistically suppress BCE-cell proliferation.

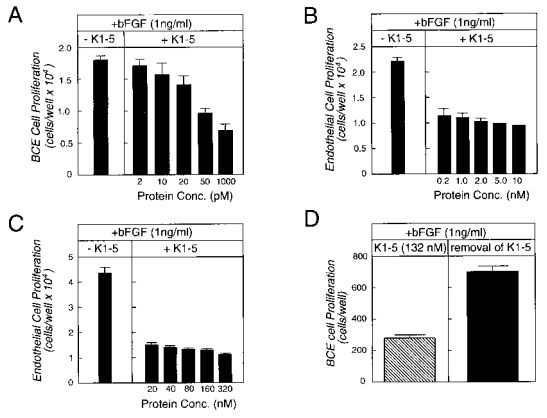

FIG. 2. Inhibition of endothelial-cell proliferation. Purified K1–5 at various concentrations was assayed on BCE cells in the presence of FGF-2 (1 ng/ml) in a 72-h proliferation experiment. (*A*) K1–5 displays a dose-dependent effect on suppression of BCE cell growth. (*B* and *C*) The maximal inhibitory activity was detected at 200 pM. Increase of concentrations does not enhance the inhibitory effect. (*D*) The inhibitory activity of K1–5 on BCE cells was reversible and endothelial cells regrew after removal of K1–5. Values represent the mean ± SEM of triplicate of each sample.

Inhibition of Angiogenesis in the CAM. To study the *in vivo* antiangiogenic activity, proteolytic human K1–5 was tested on the CAM. At concentrations of 5–25 μg per disk, K1–5 inhibited new embryonic blood vessel growth, as measured by the formation of avascular zones (Fig. 4*B*, the area marked with curved arrows). Within the avascular zone, a large number of newly formed blood vessels were regressed. The measured inhibition was dose-dependent (Fig. 4*C*) over the range of 5–25 μg per embryo, and no obvious inflammation was detected. No avascular zones were found in the control embryos implanted with disks containing PBS alone (Fig. 4 *A* and *C*). These results demonstrate that K1–5 is able to suppress angiogenesis in embryos.

Suppression of Mouse Corneal Neovascularization. To further investigate the antiangiogenic activity of K1–5 *in vivo* and to directly compare the antiangiogenic efficacy of K1–5 with that of angiostatin, the inhibitory effect of systemic administration of K1–5 and angiostatin on FGF-induced corneal neovascularization was studied. This rigorous antiangiogenic assay requires a putative angiogenesis inhibitor to be administrated systemically (e.g., subcutaneous or intraperitoneal injections) to examine its capacity to suppress 80 ng of FGF-induced corneal neovascularization. Systemic treatment of mice with K1–5 by one subcutaneous injections once daily at the concentration of 2 mg/kg significantly blocked the FGF-induced corneal neovascularization (Fig. 5*C*). The length (Fig.5*D*) and clock hours (Fig. 5*E*) of corneal circumferential neovascularization were inhibited by 50–70% in 10 corneas of five individual mice. The density of corneal vessels in the K1–5-treated animals (Fig. 5*C*) was also markedly reduced as compared with that of control animals treated with PBS (Fig. 5*A*). About 80% reduction of the area of corneal neovascularization was observed in the K1–5-treated group compared with that of the control group treated with PBS alone (Fig. 5*F*). In contrast, angiostatin at the same dose did not significantly

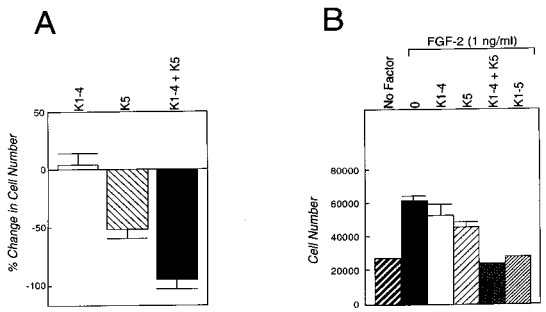

FIG. 3. Synergistic inhibition of endothelial cell proliferation by angiostatin and K5. (*A*) Angiostatin (K1–4), K5, and the combination of these two inhibitory fragments at a concentration of 1 nM were assayed on BCE cells in the presence of FGF-2 (1 ng/ml) for 72 h. Each sample was assayed as a triplicate. Values represent the mean ± SEM of three determinations as percent change of cell number. (*B*) Kringle 1–4, K5, K1–4 + K5, K1–5 at a concentration of 1 nM were added to BCE cells in the presence of FGF-2 (1 ng/ml) for 72 h. Each sample was assayed as a triplicate. Values represent the mean ± SEM of a triplicate of each sample as cell numbers. BCE cell proliferation in the presence and absence of FGF-2 served as controls.

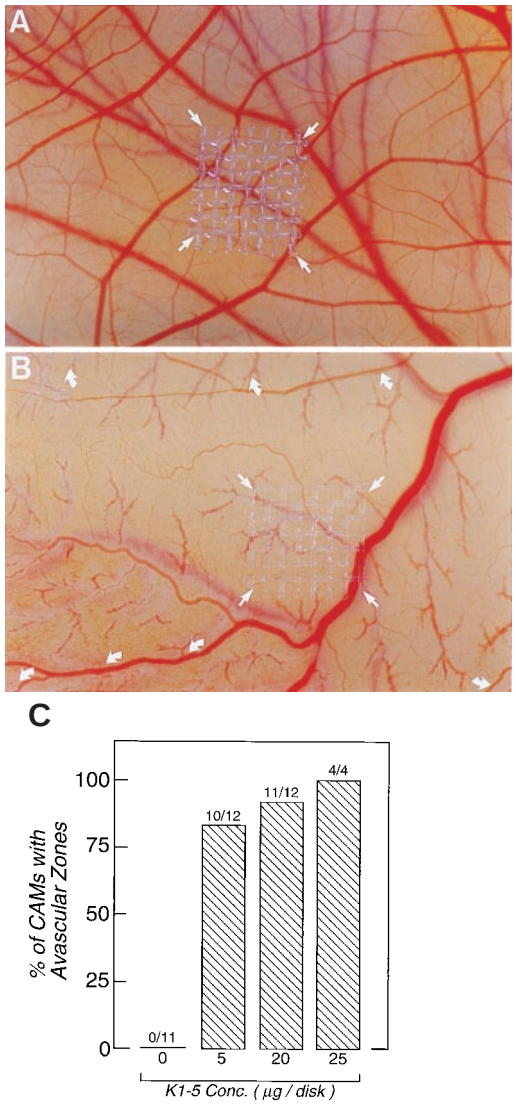

FIG. 4. Inhibition of angiogenesis by K1–5 on the CAM. Methylcellulose discs containing various amounts of K1–5 were dried on a nylon mesh (4 × 4 mm). The meshes were implanted on CAMs of 6-day chicken embryos as described (31, 32). After 48 h, the formation of avascular zones was analyzed under a stereomicroscope. (*A*) A control CAM with a methylcellulose disc (white arrows) containing PBS. (*B*) Micrograph of an example of K1–5-implanted CAM. The formation of the avascular zone is marked by curved arrows. White arrows point to the implanted disk. Restriction and regression of blood vessel growth can be observed in the avascular zone area. (*C*) The number of avascular zones over the total number of CAMs tested at various concentrations of K1–5 is indicated above each bar.

inhibit the FGF-induced corneal vascularization (Fig. 5 *B* and *D–F*) compared with the PBS-treated group (Fig. 5 *A* and *D–F*). Thus, K1–5 displayed a more potent antiangiogenic effect than K1–4 in this rigorous *in vivo* model. The treated mice did not experience weight loss or unusual behavior over the course of the treatment, indicating that K1–5 was not toxic at the dose used in our experiments.

Suppression of Primary Tumor Growth by Systemic Administration of K1–5. Because K1–5 inhibited neovascularization *in vivo* and tumor growth requires angiogenesis (8), we determined the antitumor activity of K1–5. Proteolytic human K1–5 was used to systemically treat C57BL6/J mice bearing subcutaneously implanted primary T241 fibrosarcomas. K1–5 at the dose of 2.5 mg per kg per day was subcutaneously injected once daily in the ventral abdomen of mice, whereas subcutaneous tumors were growing in the midline dorsum of each mouse. This daily systemic

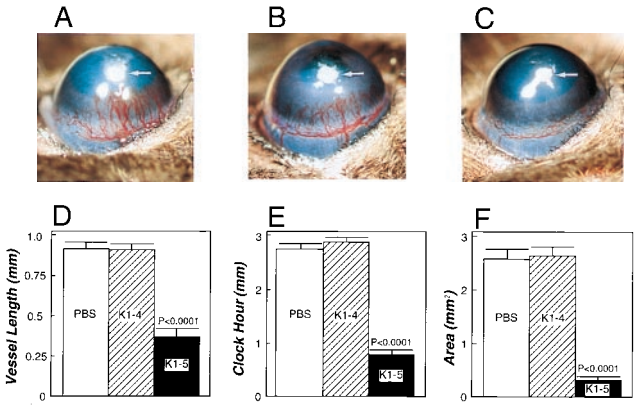

FIG. 5. Inhibition of mouse corneal neovascularization. Pellets containing sucrose aluminum sulfate, hydron, and 80 ng of FGF were implanted into corneal micropockets of mice. Corneas were photographed with a stereomicroscope on day 6 after FGF implantation and positions of implanted pellets were indicated by arrows in *A–C*. (*A*) Cornea of a control mouse receiving daily subcutaneous injection of PBS. (*B*) An example of the mouse cornea treated with daily subcutaneous injections of K1–4 (2 mg/kg). (*C*) An example of the mouse cornea treated with daily subcutaneous injections of K1–5 (2 mg/kg). Five mice of each treated and control group were used. (*D*) Maximal vessel length. (*E*) Clock hours of circumferential neovascularization. (*F*) Area of neovascularization. All data in *D–F* are presented as the mean ± SEM from 10 corneas in each group.

administration of K1–5 resulted in a significant suppression of the growth of primary tumors during the 20-day treatment course (Fig. 6). At day 20 after treatment, an average of over 65% suppression of primary tumor growth was observed in the K1–5-treated mice ($n = 5$). In contrast, tumors grew rapidly to sizes >7500 mm^3 in the saline-treated animals ($n = 5$) during the same 20-day treatment period (Fig. 6*B*), leading to the demise of all mice within 5 weeks after tumor implantation. The K1–5-treated mice showed no weight loss or unusual behavior over the course of treatment.

To directly compare the antitumor efficacy of K1–5 with that of angiostatin, we performed the side-by-side comparison experiment by using the same tumor model system. As shown in Fig. 7, systemic treatment of K1–5 at the concentration of 2 mg/kg, once daily, again significantly suppressed the growth of T241 fibrosarcoma in syngeneic C57BL6/J mice ($n = 5$) by approximately 63% compared with the control group treated with PBS ($n = 5$). In contrast, angiostatin at the same dose did not significantly block tumor growth ($n = 5$) when compared with the PBS-treated group during the 18-day treatment course. We should emphasize that although K1–5 significantly inhibited tumor growth, it did not completely arrest tumors at a dormant stage. The K1–5-treated tumors would eventually but at a delayed rate grow to large sizes that were comparable to the control tumors treated with PBS or angiostatin.

Suppression of Tumor Neovascularization. To evaluate the suppressive effect of K1–5 on tumor angiogenesis, tumor tissue sections were immunohistochemically stained with an endothelial specific antibody against von Willebrand factor and microvessels in tumor tissues were randomly counted. Primary tumors were resected at day 20 after systemic treatment with K1–5. A dramatically decreased microvessel density in tumor tissues was revealed in the K1–5-treated mice (Fig. 8 *B–D*) compared with control tumor tissues treated with PBS ($P < 0.001$) (Fig. 8 *A* and *D*). Fig. 6*D* represented an average of vessel density of six randomly selected fields in tumors from three mice of each group.

DISCUSSION

The present study demonstrates that proteolysis of Pgn triggered by plasmin leads to generation of a potent angiogenesis inhibitor, K1–5. *In vitro*, K1–5 specifically inhibits capillary endothelial-cell

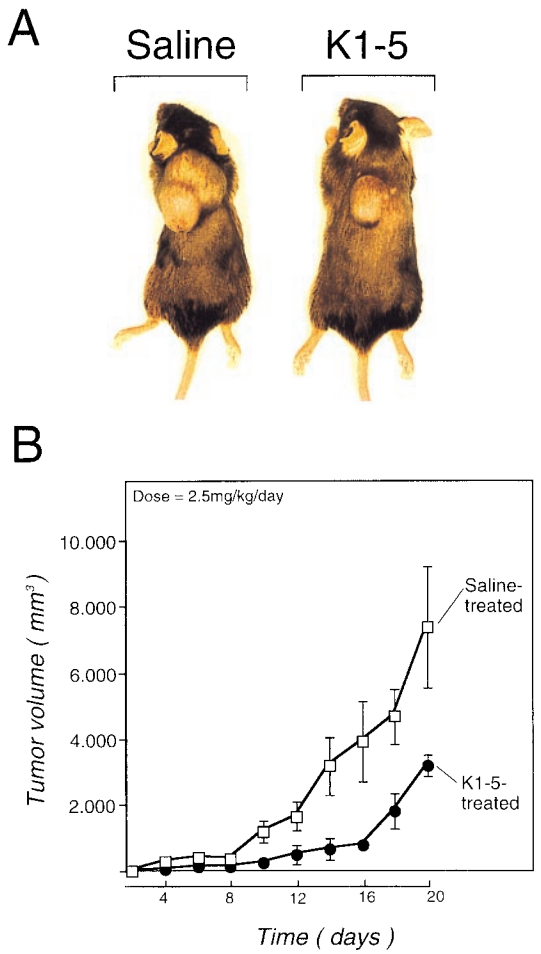

FIG. 6. Suppression of tumor growth in syngeneic C57BL6/J. Male C57BL6/J syngeneic mice were subcutaneously implanted with 1×10^6 T241 tumor cells per mouse and systemically treated with K1–5 by subcutaneous injections in the abdomen at the dose of 2.5 mg/kg once daily from day 0 through day 20. (*A*) Graphs of T241 fibrosarcoma-bearing mice treated with PBS (*Left*) and K1–5 (*Right*) at day 20 after treatment. (*B*) Tumor volumes of K1–5-treated group (●) vs. control saline-treated group (□) on days indicated. Data represent the tumor volume (mean ± SEM) from four or five mice in each group.

growth, but has no effect on several nonendothelial cell types including primary human fibroblasts, retinal pigment epithelial cells, rodent fibroblasts, rodent smooth muscle cells, and tumor cells. It potently blocks neovascularization and tumor growth *in vivo*. A significant reduction (>70%) of microvessel density was

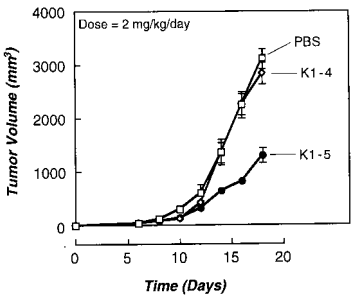

FIG. 7. Comparison of the antitumor effect of K1–5 with that of angiostatin. Male C57BL6/J syngeneic mice were subcutaneously implanted with 1×10^6 T241 tumor cells per mouse and systemically treated with K1–5 by subcutaneous injections in the abdomen at the dose of 2 mg/kg once daily from day 0 through day 18. Tumor volumes of K1–5-treated group (●) vs. control saline-treated group (□) and angiostatin-treated group (◇) on days indicated. Data represent the tumor volume (mean ± SEM) of five mice in each group.

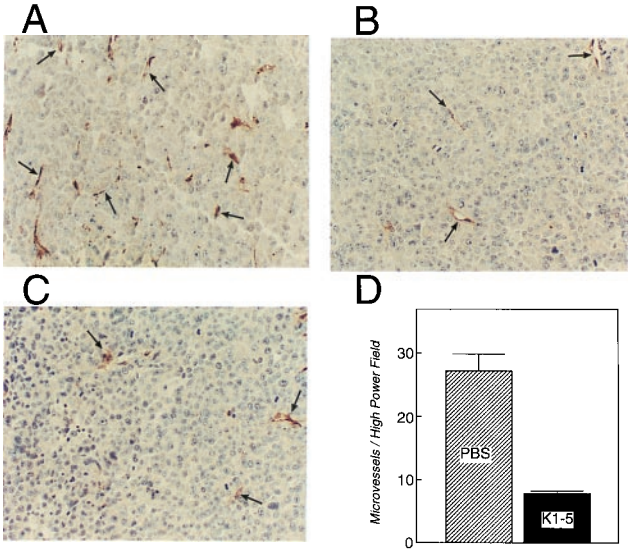

FIG. 8. Immunohistochemical analysis of neovascularization of primary tumors. T241 tumor bearing C57BL6/J mice were systemically treated with K1–5 (*B* and *C*) and control saline (*A*), and primary tumors were resected on day 20 after treatment. Tumor histological sections were stained with a polyclonal antibody against von Willebrand factor. Neovascularization of tumors was revealed by the antibody (brown staining pointed to by arrows). (*D*) Microvessel density per high-power field (×40) of K1–5-treated (solid bar) and saline-treated (hatched bar). Data are the mean ± SEM. Microvessels were counted from six randomly selected fields in tumors from three mice of each group. The values are significantly different ($P < 0.0001$).

found in tumors from the animals treated with K1–5 compared with that of control tumors. Thus, the antitumor effect of K1–5 is mediated via the antiangiogenic pathway.

Pgn contains five kringle structures in total followed by a serine protease module (23). Angiostatin, a potent angiogenesis inhibitor, encompasses the first four kringle domains of Pgn. Angiostatin was first discovered in mice as a proteolytic fragment generated in association with murine 3LL Lewis lung carcinoma growth (5). A recent study shows that metalloelastase (MME) produced by tumor-infiltrating macrophages is responsible for the *in vivo* production of angiostatin in syngeneic C57BL6/J mice bearing Lewis lung carcinomas (37). In addition to MME, three human prostate carcinoma cell lines (PC-3, DU-145, and LN-CaP) have been reported to produce a serine protease that can convert Pgn into angiostatin (35). It is not known, however, whether K1–5 can also be produced in association with tumor growth. If so, what proteolytic enzymes are involved in conversion of Pgn to K1–5. *In vivo*, several proteolytic enzymes including elastase (5, 17) stromelysin 1 (MMP-3) (38), human matrilysin (MMP-7) (39), gelatinase B (39), and type IV collagenase (MMP-9) (39) have recently been reported to convert Pgn to angiostatin. Plasmin has also been reported for generation of angiostatin under a reducing condition (36). These studies demonstrate that several proteases participate in conversion of the same precursor molecule into a common angiogenesis inhibitor. To date, little is known about the regulation of the proteolytic activity of these angiostatin-converting enzymes *in vivo*. Further, we do not know the tissue-specific activity of each protease and the substrate specificity under physiological and pathological conditions.

Limited proteolysis of Pgn by elastase and pepsin leads to the generation of another potent endothelial growth inhibitor, K5. In fact, K5 in cell culture appears to be more potent in suppression of endothelial-cell growth than angiostatin (Fig. 3) (23). Further, elastase digestion of Pgn can also generate K1–3, which seems to be at least as potent as angiostatin in suppression of endothelial cell growth (17). These findings suggest that several angiostatic fragments can be produced from the proteolytic degradation of

Pgn and that all angiostatic fragments contain kringle domains. In regard to molecular mechanisms underlying the angiostatic actions of the kringle structures, little knowledge has been gained since the discovery of angiostatin. Recently, angiostatin has been reported to increase endothelial-cell apoptosis and the activity of focal adhesion kinase (40). It appears that K5 may act through a separate pathway because angiostatin and kringle 5 synergistically suppress endothelial cell growth *in vitro* and K1–5 could simultaneously activate both pathways because its endothelial inhibitory effect is comparable with that of angiostatin plus K5. It is not known whether angiostatin and K5 use different endothelial receptors to transduce their inhibitory effects. Further, we do not know whether there are any endothelial-specific receptors for angiostatin or K5 because other molecules can also mediate endothelial cell signals, such as integrins (6). The mechanisms of the inhibitory effects of K5 and K1–5 remain to be investigated.

Proteolytic enzymes including urokinase and plasmin have been reported to participate in the invasion of tumor cells into neighboring tissues and cancer metastasis (41). They are also involved in positive regulation of angiogenesis. For example, the urokinase–plasmin system may be important for endothelial cells at the initial step of angiogenesis to degrade the surrounding basement membrane for endothelial cells to penetrate into surrounding tissues (4). In addition, plasmin can release growth factors such as vascular endothelial growth factor and FGF, which are sequestered in the extracellular matrix (42). It can also convert the latent form of transforming growth factor β into the active form, which may indirectly stimulate angiogenesis *in vivo* (43). Our present study provides evidence that the urokinase-plasmin system may down-regulate angiogenesis by generation of a potent angiogenesis inhibitor, K1–5. Thus, plasmin plays dual roles in the control of the process of angiogenesis depending upon different phases of the vasculature development. At the beginning of angiogenesis, the urokinase–plasmin system may be required for the formation of vessel sprouts. The same system may also be used to switch off angiogenesis by producing angiogenesis inhibitors such as K1–5 to prevent the overgrowth of blood vessels.

Apparently, the urokinase–plasmin system is not the only system that operates the switch of angiogenesis. Several others of the known angiogenesis inhibitors are also proteolytic fragments of large precursor proteins. These include endostatin, the 16-kDa N-terminal fragment of prolactin, PEX (a noncatalytic metalloprotease fragment), a proteolytic fibronectin fragment, and a proteolytic fragment with the N-terminally truncated sequence of platelet factor-4 (22). Comparison of amino acid sequences of cleavage sites of these angiogenesis inhibitors does not reveal a common cleavage site (22), suggesting that more than one protease are involved in the generation of various angiogenesis inhibitors. Thus, generation of endogenous inhibitors from large precursor proteins is a recurrent theme in suppression of angiogenesis.

Systemic treatment of tumor-bearing mice with high doses (50–100 mg/kg, two times a day) of angiostatin has been shown to prevent tumor growth and metastasis (5, 7). However, potential therapeutic applications of this angiogenesis inhibitor for cancer patients may become problematic because large amounts of angiostatin are needed for therapy. Thus, to improve the potency of the antiangiogenic effect, to extend the *in vivo* half-life, to develop a slow release strategy, and to establish a gene therapy approach are urgently demanded for the angiostatic therapy. K1–5 seems to be a better candidate that may fulfill some of these criteria. It displays a more potent effect on suppression of endothelial-cell growth, angiogenesis, and tumor growth than angiostatin. It has a longer half-life in the body than angiostatin due to its increased molecular weight (unpublished data). Importantly, K1–5 significantly reduces tumor growth in mice at a low dose at which angiostatin is ineffective. We should emphasize that K1–5 did not completely arrest tumor growth in our animal model system. Increase of doses of K1–5 did not arrest tumors at a dormant stage either. However, it significantly reduces the rate of tumor growth. Therefore, K1–5 may become useful for potential clinical treatment of cancer patients and for treatment of other angiogenic diseases.

We thank Kristin Ottarsdottir and Ulla Aspenblad for their technical assistance. We also thank Anna Eriksson for critical reading of the manuscript. Y.C. is supported by the Swedish Medical Research Council, Grant K97-12P-11819-02B. This work was supported by the Swedish Medical Research Council Grant K97-12X-12185-01A to Y.C., the Swedish Cancer Foundation Grant 3811-B96-01XAB (961607) to Y.C., and the Fredrik and Ingrid Thurings Foundation, the Karolinska Institute Foundation, the Magnus Bergvalls Foundation and the Harold Jeanssons Foundation.

1. Folkman, J. & Shing, Y. (1992) *J. Biol. Chem.* **267,** 10931–10934.
2. Folkman, J. & D′Amore, P. (1996) *Cell* **87,** 1153–1155.
3. Risau, W. (1997) *Nature (London)* **386,** 671–674.
4. Hanahan, D. & Folkman, J. (1996) *Cell* **86,** 353–364.
5. O'Reilly, M. S., Holmgren, L., Shing, Y., Chen, C., Rosenthal, R. A., Moses, M., Lane, W. S., Cao, Y., Sage, E. H. & Folkman, J. (1994) *Cell* **79,** 315–328.
6. Brooks, P. C., Montgomery, A. M., Rosenfeld, M., R. A., R., Hu, T., Klier, G. & Cheresh, D. A. (1994) *Cell* **79,** 1157–1164.
7. O'Reilly, M. S., Holmgren, L., Chen, C. & Folkman, J. (1996) *Nat. Med.* **2,** 689–692.
8. Folkman, J. (1995a) *Nat. Med.* **1,** 27–31.
9. Good, D. J., Polverini, P. J., Rastinejad, F., LeBeau, M. M., Lemons, R. S., Frazier, W. A. & Bouck, N. P. (1990) *Proc. Natl. Acad. Sci. USA* **87,** 6624- 6628.
10. Kim, K. J., Li, B., Winer, J., Armanini, M., Gillett, N., Phillips, H. S. & Ferrara, N. (1993) *Nature (London)* **362,** 841–844.
11. Kandel, J., Bossy-Wetzel, E., Radvanyi, F., Klagsbrun, M., Folkman, J. & Hanahan, D. (1991) *Cell* **66,** 1095–1104.
12. Senger, D. R., Galli, S. J., Dvorak, A. M., Perruzzi, C. A., Harvey, V. S. & Dvorak, H. F. (1983) *Science* **219,** 983–985.
13. Ferrara, N. & Davis-Smyth, T. (1997) *Endocr. Rev.* **18,** 4–25.
14. Nguyen, M., Watanabe, H., Budson, A. E., Richie, J. P., Hayes, D. F. & Folkman, J. (1994) *J. Natl. Cancer Inst.* **86,** 356–361.
15. Mustonen, T. & Alitalo, K. (1995) *J. Cell Biol.* **129,** 895–898.
16. Pepper, M. S., Ferrara, N., Orci, L. & Montesano, R. (1992) *Biochem. Biophys. Res. Commun.* **189,** 824–831.
17. Cao, Y., Ji, R.-W., Davidson, D., Schaller, J., Marti, D., Sohndel, S., McCance, S. G., O'Reilly, M. S., Llinas, M. & Folkman, J. (1996) *J. Biol. Chem.* **271,** 29461–29467.
18. Holmgren, L., O'Reilly, M. S. & Folkman, J. (1995) *Nat. Med.* **1,** 149–153.
19. O'Reilly, M. S., Boehm, T., Shing, Y., Fuhai, N., Vasios, G., Lane, W. S., Flynn, E., Birkhead, J. R., Olsen, B. & Folkman, J. (1997) *Cell* **88,** 1–20.
20. Boehm, T., Folkman, J., T., B. & O'Reilly, M. S. (1997) *Nature (London)* **390,** 335- 336.
21. Volpert, O. V., Lawler, J. & Bouck, N. P. (1998) *Proc. Natl. Acad. Sci. USA* **95,** 6343–6348.
22. Cao, Y. (1998) *Progress in Molecular and Subcellular Biology- Inhibitors of Cell Growth* (Springer, Berlin; Heidelberg; London; New York), Vol. 20, pp. 161–176.
23. Cao, Y., Chen, A., An, S. S. A., Ji, R. W. D., Davidson, D., Cao, Y. M. & Llinas, M. (1997) *J. Biol. Chem.* **272,** 22924–22928.
24. Clapp, C., Martial, J. A., Guzman, R. C., Rentierdelrue, F. & Weiner, R. I. (1993) *Endorinology* **133,** 1292–1299.
25. Gupta, S. K., Hassel, T. & Singh, J. P. (1995) *Proc. Natl. Acad. Sci. USA* **92,** 7799- 7803.
26. Brooks, P. C., Silletti, S., Schalscha, T. L., Friedlander, M. & Cheresh, D. (1998) *Cell* **92,** 391–400.
27. Cao, Y., O′Reilly, M. S., Marshall, B., Flynn, E., Ji, W. R. & Folkman, J. (1998) *J. Clin. Invest.* **101,** 1055–1063.
28. Cao, Y. & Pettersson, R. F. (1990) *Growth Factors* **3,** 1–13.
29. Wu, H. L., Chang, B. I., Wu, D. H., Chang, L. C., Gong, C. C., Lou, K. L. & Shi, G. Y. (1990) *J. Biol. Chem.* **265,** 19658–19664.
30. Folkman, J., Haudenschild, C. C. & Zetter, B. R. (1979) *Proc. Natl. Acad. Sci. USA* **76,** 5217–5121.
31. Cao, Y., Chen, C., Weatherbee, J. A., Tsang, M. & Folkman, J. (1995) *J. Exp. Med.* **182,** 2069–2077.
32. Nguyen, M., Shing, Y. & Filkman, J. (1994) *Microvascular Res.* **47,** 31–40.
33. Kenyon, B. M., Voest, E. E., Chen, C., Flynn, E., Folkman, J. & D'Amato, R. J. (1996) *Invest. Ophthal. Visual Sci.* **37,** 1625–1632.
34. Jain, R. K., Schlenger, K., Hockel, M. & F., Yuan. (1997) *Nat. Med.* **3,** 1203–1208.
35. Gately, S., Twardowski, P., Stack, M. S., Patrick, M., Boggio, L., Cundiff, D. L., Schnaper, H. W., Madison, L., Volpert, O., Bouck, N., *et al.* (1997) *Cancer Res.* **56,** 4887–4890.
36. Stathakis, P., Fitzgerald, M., Matthias, L. J., Chesterman, C. N. & Hogg, P. J. (1997) *J. Biol. Chem.* **272,** 20641–20645.
37. Dong, Z., Kumar, R., Yang, X. & Fidler, I. J. (1997) *Cell* **88,** 801–810.
38. Lijnen, H. R., Ugwu, F., Bini, A. & Collen, D. (1998) *Biochemistry* **37,** 4699–4702.
39. Patterson, B. C. & Sang, Q. X. A. (1997) *J. Biol. Chem.* **272.**
40. Claesson-Welsh, L., Welsh, M., Ito, N., Anandapte, B., Soker, S., Zetter, B., O'Reilly, M. & Folkman, J. (1998) *Proc. Natl. Acad. Sci. USA* **95,** 5579–5583.
41. Evans, C. P., Elfman, F., Parangi, S., Conn, M., Cunha, M. & Shuman, M. A. (1997) *Cancer Res.* **57,** 3594–3599.
42. Plouet, J., Moro, F., Bertagnolli, S., Coldeboeuf, N., Mazarguil, H., Clamens, S. & F., B. (1997) *J. Biol. Chem.* **272,** 13390–13396.
43. Nakanishi, Y., Kodama, J., Yoshinouchi, M., Tokumo, K., Kamimura, S., Okuda, H. & Kudo, T. (1997) *Int. J. Gynecol. Pathol.* **16,** 256–262.